Neurobiology of Stress 19 (2022) 100466

Contents lists available at ScienceDirect

Neurobiology of Stress

journal homepage: www.elsevier.com/locate/ynstr

Chronic hypothalamic-pituitary-adrenal axis disruption alters glutamate homeostasis and neural responses to stress in male C57Bl6/N mice

Scott A. Kinlein [a], Naomi K. Wallace [a], Marina I. Savenkova [a], Ilia N. Karatsoreos [a,b,*]

[a] Dept. of Integrative Physiology and Neuroscience, Program in Neuroscience, Washington State University, Pullman, WA, 99164, USA
[b] Dept. of Psychological and Brain Science, Neuroscience and Behavior Program, University of Massachusetts – Amherst, Amherst, MA, 01003, USA

ARTICLE INFO

Keywords:
Frontal cortex
Hippocampus
Amygdala
Stress response
Vulnerability
Excitatory neurotransmission

ABSTRACT

It is now well-established that stress elicits brain- and body-wide changes in physiology and has significant impacts on many aspects of health. The hypothalamic-pituitary-adrenal (HPA) axis is the major neuroendocrine system mediating the integrated response to stress. Appropriate engagement and termination of HPA activity enhances survival and optimizes physiological and behavioral responses to stress, while dysfunction of this system is linked to negative health outcomes such as depression, anxiety, and post-traumatic stress disorder. Glutamate signaling plays a large role in the transmission of stress-related information throughout the brain. Furthermore, aberrant glutamate signaling has negative consequences for neural plasticity and synaptic function and is linked to stress-related pathology. However, the connection between HPA dysfunction and glutamate signaling is not fully understood. We tested how HPA axis dysfunction (using low dose chronic corticosterone in the drinking water) affects glutamate homeostasis and neural responses under baseline and acute stress in male C57BL/6N mice. Using laser microdissection and transcriptomic analyses, we show that chronic disruption of the HPA axis alters the expression of genes related to glutamate signaling in the medial prefrontal cortex (mPFC), hippocampus, and amygdala. While neural responses to stress (as measured by FOS) in the hippocampus and amygdala were not affected in our model of HPA dysfunction, we observed an exaggerated response to stress in the mPFC. To further probe this we undertook *in vivo* biosensor measurements of the dynamics of extracellular glutamate responses to stress in the mPFC in real-time, and found glutamate dynamics in the mPFC were significantly altered by chronic HPA dysfunction. Together, these findings support the hypothesis that chronic HPA axis dysfunction alters glutamatergic signaling in regions known to regulate emotional behavior, providing more evidence linking HPA dysfunction and stress vulnerability.

1. Introduction

Stress can be defined as any threat, real or perceived, to an organism's well-being. Exposure to these threats results in physiological changes in both the periphery and central nervous system which enable the organism to appropriately cope with the situation and ensure that the organism is better adapted to cope with similar threats in the future. Inappropriate responses to stress, or an inability to adapt to stress over time, have significant consequences for an organism's well-being and survival, leading to increased allostatic load and eventually overload (McEwen, 1998). In addition to existential issues related to improper responses to physical danger, the consequences of poor stress adaptation are evidenced in clinical disorders such as major depressive disorder and post-traumatic stress disorder, and in related disorders such as obesity and autoimmune disease. All of these pathological states include dysfunction of the stress response as a predisposing factor (McEwen, 1998; de Kloet et al., 2006; Pariante and Lightman, 2008; Bose et al., 2009; Harbuz, 2002).

The hypothalamic-pituitary-adrenal (HPA) axis is a neuroendocrine system which regulates neurobehavioral responses to stress exposure as well as adaptation to repeated or prolonged threats over time. Initiation of the HPA axis response to stress occurs in the paraventricular nucleus of the hypothalamus (PVH), with excitation of corticotropin-releasing hormone (CRH)-containing neurons causing the release of CRH into the median eminence, reaching the anterior pituitary via the hypophyseal portal system. Pituitary corticotrophs then secrete

* Corresponding author. Neuroscience and Behavior Program Department of Psychological and Brain Sciences, Tobin Hall, 135 Hicks Way, Amherst, MA, 01003, USA.
E-mail address: ikaratsoreos@umass.edu (I.N. Karatsoreos).

https://doi.org/10.1016/j.ynstr.2022.100466
Received 21 March 2022; Received in revised form 26 May 2022; Accepted 2 June 2022
Available online 5 June 2022

adrenocorticotropic hormone (ACTH) into the bloodstream, stimulating glucocorticoid production and secretion from the adrenal gland (Herman et al., 2016; Ulrich-Lai and Herman, 2009). Glucocorticoids, including corticosterone (CORT), exert rapid actions on peripheral metabolism and neuronal function as well as protracted actions on these processes through changes in gene transcription (Datson et al., 2008; Joels et al., 2012).

Glucocorticoids can cause structural and functional changes in many parts of the brain known to mediate stress responses. Of the brain regions affected by stress, the medial prefrontal cortex (mPFC), hippocampus, and amygdala are amongst the most well studied as they play clear roles in behavioral and emotional responses to stress (McEwen and Morrison, 2013; Kim et al., 2015; Ressler, 2010). Chronic exposure to stress or glucocorticoids induces divergent structural changes in neurons of these brain regions, with dendritic atrophy observed in the mPFC and hippocampus and dendritic hypertrophy observed in the amygdala (McEwen et al., 2015, 2016). A leading hypothesis for the cause of these effects is that these changes occur because of changes in synaptic excitability that, if left unconstrained, can lead to excitotoxic neuronal damage (Popoli et al., 2011; Sanacora et al., 2012).

Glutamate signaling is the main form of excitatory synaptic communication in the brain and is involved in a multitude of processes underpinning synaptic plasticity (Erecinska and Silver, 1990; Meldrum, 2000; Luscher and Malenka, 2012). The ability of glutamate to increase excitability of a synapse is regulated by ionotropic and metabotropic glutamate receptors as well as astrocytic mechanisms of glutamate transport and metabolism. Dysregulation in glutamate signaling is a leading hypothesis in the development of stress-related mood disorders such as depression, and glutamate signaling molecules are major targets of pharmacological treatments for such disorders (Popoli et al., 2011; Sanacora et al., 2012; Musazzi et al., 2012). Since glucocorticoids affect aspects of glutamate signaling, and dysregulation of the HPA axis is a major risk factor for the development of these disorders, it is necessary to determine what functional links may exist between HPA dysregulation and changes in glutamate signaling in the brain. However, there are currently few studies published which evaluate the effects of chronic HPA dysfunction on glutamate signaling or related stress-induced neural function.

In this study, we disrupted normal HPA axis function via chronic oral administration of CORT in the drinking water of mice, and characterized both basal change in gene expression, and neural responses to acute stress exposure. This model of HPA axis disruption has benefits over traditionally used methods such as adrenalectomy, as it blunts hypothalamic CRH, pituitary ACTH, and adrenal CORT while leaving the adrenal intact (Kinlein et al., 2015). An additional benefit is the maintenance of a diurnal CORT rhythm, the absence of which is known to have its own negative effects (Dedovic and Ngiam, 2015). The goals of this study were to determine how chronic dysfunction of the HPA axis affects 1) adaptation of the glutamate system in the prefrontal cortex, hippocampus, and amygdala as measured by gene expression; 2) stress-induced neural activity in these regions as measured by FOS immunoreactivity; and 3) stress-induced extracellular glutamate release measured in real time by in-vivo amperometric biosensors. Our results demonstrate that chronic HPA disruption causes changes in the expression of genes related to glutamate signaling and synaptic homeostasis differentially across the medial prefrontal cortex (mPFC), dorsal hippocampal dentate gyrus (DG), and basolateral amygdala (BLA). We further show that despite changes in gene expression in all three brain regions, stress-induced FOS immunoreactivity is exaggerated only in the mPFC. Finally, using state-of-the-art *in vivo* biosensors with very high temporal resolution, we show that extracellular glutamate responses to stress are altered following chronic HPA disruption, suggesting that increased FOS responses to stress in the mPFC could be driven by altered glutamate release or extracellular glutamate clearance. Together, these results demonstrate that chronic dysfunction of the HPA axis alters glutamatergic signaling in the brain, and potentially impacts stress-induced synaptic excitability.

2. Methods

2.1. Animals and corticosterone treatment

Our overall experimental design is provided in Fig. 1. Adult male mice C57BL/6N mice were obtained from Envigo (Livermore, CA). Upon arrival, mice were group-housed (4 per cage) in standard cages on a 12-h light-dark cycle (lights on at 5:00 h, ~100lux) and given access to standard rodent chow and drinking water *ad libitum*. For *in-vivo* glutamate recording experiments, mice were single housed in the same conditions. To disrupt normal HPA function, after 7 days of acclimation to the facility, chow remained available, while drinking water was replaced with solution containing 25 μg/mL CORT (Sigma Inc., St. Louis, MO, HPA-X group) dissolved in 100% ethanol, and then diluted in regular drinking water to a final concentration of 1% ethanol (Vehicle, Control group). CORT or Vehicle treatments were administered for 4 weeks in all experiments, with treatment solutions being replaced weekly during cage changes. This dose and duration of CORT treatment is based on previous studies from our lab and others that show this dosage and duration maintains a diurnal pattern of plasma CORT (albeit at a higher peak level of 90 ng/ml, but an unchanged nadir at ~20 ng/ml), results in blunted hypothalamic CRH mRNA as well as blunted stress-induced ACTH and CORT (Kinlein et al., 2015; Shahanoor et al., 2017). On the day of stress exposure or tissue collection, water bottles containing VEH or CORT were removed from all cages 1hr prior to testing so as to prevent any potential confounds from CORT consumption just prior, as previously undertaken (Kinlein et al., 2015).

2.2. Experiment 1

To test how glutamate homeostasis is affected by chronic HPA axis dysfunction, following 4-week CORT or Vehicle exposure, mice (N = 8/group; 16 total) were euthanized via rapid decapitation in unstressed conditions at 11:00 h (6 h after lights on, Zeitgeber Time (ZT)6), and brains collected and snap frozen on dry ice for gene expression analysis. Brains were stored at −80 °C until laser microdissection was performed.

2.3. Experiment 2

To test how stress-induced neural activity is affected by chronic HPA axis dysfunction, following 4-week CORT or Vehicle exposure, mice (N = 8/group, 32 total) were exposed to a single forced swim stress (10 min, 21–23 °C) between 10:00–12:00 h (5–7 h after lights on, ZT5-7). Following swim stress, mice were briefly dried with paper towels and placed back into home cages in the animal housing room. One hour after the start of stress (or without manipulation in the unstressed groups), mice were anaesthetized with ketamine (15 mg/ml)/xylazine (1 mg/ml) cocktail and then transcardially perfused with heparinized saline and 4% paraformaldehyde. Brains were then collected and processed for immunohistochemical analysis.

2.4. Experiment 3

To determine how stress-induced glutamate release is affected by chronic HPA axis disruption, mice (N = 10/group, 20 total) were implanted with printed circuit board (PCB) head stages as previously described (Phillips et al., 2015; Wallace et al., 2020) (Pinnacle Technology, Inc., Lawrence, KS) with an additional cannula targeted to the mPFC under isoflurane anesthetic (details below). Following 7 days of recovery from surgery, mice began 4-week treatment with CORT or Vehicle solution. On day 26 of treatment, mice were placed in biosensor recording chambers for a 24 h acclimation period, after which glutamate biosensors (Pinnacle) were implanted on day 27 and extracellular glutamate was recorded continuously at a rate of 1hz for the remainder

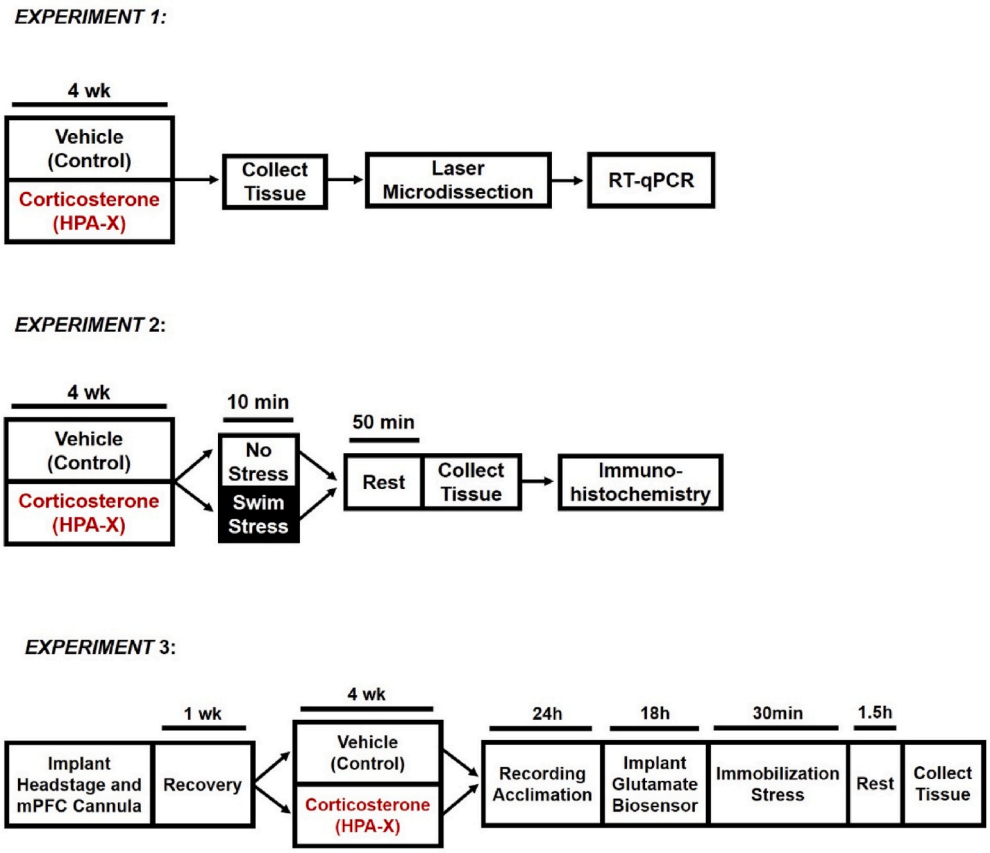

Fig. 1. Experimental designs for experiments 1, 2, and 3. For all experiments, corticosterone (CORT, 25 μg/mL, HPA-X) or Vehicle (1% EtOH, Control) solutions were administered orally in drinking water.

of the experiment. On day 28, 18 h after biosensor implantation at 11:00 h (ZT6), mice were exposed to immobilization stress for 30min in plastic decapicone tubes (Braintree Scientific, Inc., Braintree, MA). Glutamate was recorded throughout the stress period and for 1.5 h during the recovery period after the end of stress exposure. Following biosensor recordings, mice were returned to their home cage and euthanized within 24 h via rapid decapitation. Cannula were then heated with a soldering iron at 720 °C to mark the biosensor recording area and brains were extracted and snap frozen on dry ice for later verification of cannula placement.

2.5. Laser microdissection

To determine the expression of genes related to glutamate homeostasis following HPA axis disruption, frozen brains from *Experiment 1* were sliced at 25 μm on a cryostat microtome and mounted onto membrane slides (Leica, Wetzlar, Germany). Slices were immediately stained using a fast Cresyl violet protocol as described by Leica, and then tissue from the prelimbic mPFC (bregma +1.94 to +1.54 mm A-P), dorsal DG (bregma −1.58 to −2.06 mm A-P), and BLA (bregma −1.06 to −1.46 mm A-P) (Franklin and Paxinos, 2007) were dissected from slices using a Leica Laser Microdissection LMD7 microscope. Tissue was dissected from 6–8 slices per brain region, immediately collected into Qiazol lysis reagent (Qiagen, Hilden, Germany) and stored at −80 °C until RNA isolation was performed. Average dissected areas for the mPFC, DG, and BLA were 353,827 μm^2, 255,385 μm^2 and 269,859 μm^2, respectively.

2.6. Tissue processing, immunohistochemistry, and confocal microscopy

Following extraction, brains from *Experiment 2* were post-fixed with 4% paraformaldehyde for 24-h, and then incubated in one step each of 20% and 30% sucrose in 0.1 M PB for 24-h. Brains were then sectioned at 40 μm on a cryostat microtome, and sections containing the mPFC (bregma +1.94 to +1.54 mm A-P), dorsal DG (bregma −1.58 to −2.06 mm A-P), and BLA (bregma −1.06 to −1.46 mm A-P) (Franklin and Paxinos, 2007) underwent immunohistochemical processing. Briefly, tissue sections were washed in 0.1 M PB followed by a 1-h incubation in 2% normal donkey serum (NDS) in 0.1 M PB with 0.1% Triton X-100 (PBT, Sigma). Next, tissue sections were incubated for 48 h at 4 °C in goat anti-Fos (1:4000, Santa Cruz Biotechnology, Dallas, TX, sc-52-G). Tissue sections were then washed in 0.1 M PBT and incubated for 1 h at room temperature in donkey anti-goat Alexa Fluor 591 (1:200, Jackson ImmunoReseach laboratories, Inc., West Grove, PA), followed by a final wash in 0.1 M PB. The tissue sections were then mounted on gelatin-coated glass slides and then incubated in 50%, 70%, 95% (x2), and 100% (x2) ethanol for 5 min each, followed by clearing agent (Fisher Scientific, Waltham, MA) for 5 min, and cover slipped with DPX (Sigma).

Images were captured using a Leica SP5 confocal microscope at 10X magnification for FOS quantification. For mPFC FOS quantification, the dorsal edge of the images began 750 μm from the dorsal surface of the brain and extended approximately 1000 μm ventrally. These imaging parameters allow for the unilateral capture of the medial-lateral and dorsal-ventral extent of the prelimbic mPFC, while minimizing the presence of the more dorsal anterior cingulate region of the cortex. For the DG and BLA, the entire regions were captured unilaterally in the center of view based on anatomical delineations of these regions. All imaging parameters were based on measurements from a stereotaxic brain atlas (Franklin and Paxinos, 2007).

2.7. Semi-automated FOS analysis

For quantification of FOS-positive cells in the mPFC, DG, and BLA, a semi-automated workflow was performed in ImageJ software (National Institutes of Health). After opening images, the "Z Project … [Max Intensity]" option was applied, following which the contour of each region was created by the experimenter using the "Polygon" tool. Following the creation of contours, a brightness threshold was applied to the images to reduce background fluorescence. Threshold values were determined for each image by multiplying the measure of the mean gray value by 1.7. This threshold correction was determined by the experimenter prior to data analysis by adjusting the brightness threshold to the point where the only visible cell profiles were fully-labeled FOS-positive cells in the "Control + stress" group. After adjusting the brightness threshold in each image, the "Smooth", "Watershed", and "Despeckle" options were applied to facilitate accurate quantification of FOS-positive cells. Quantification of FOS-positive cells was accomplished using the "Analyze Particles" tool, with the options as follows: size = 25–150 μm, circularity = 0.50–1.00. Total number of cells detected was then divided by the area of the respective contour to determine FOS-positive cell density. Average contour areas for the mPFC, DG, and BLA were 353,827 μm^2, 255,385 μm^2, and 269,859 μm^2, respectively. For all brain regions, 1–2 brain slices were imaged from each animal, and FOS immunofluorescence measurements were averaged between slices for analysis.

2.8. Real time qPCR

To determine how chronic HPA disruption affects glutamate homeostasis in the mPFC, DG, and BLA, mRNA was quantified via RT-qPCR. After tissue collection (see *Laser Microdissection* above), mRNA was isolated using Qiazol extraction and RNeasy Micro Kit on a QIAcube robotic workstation (Qiagen). mRNA concentration and quality were assessed using spectrophotometry by A260/A280 ration value (>1.9) as well as by RNA fragmentation analysis (RQN>7) performed on Agilent 5200 fragment analyzer. cDNA synthesis was performed with MultiScribe™ MuLV reverse-transcriptase following the High-Capacity cDNA Synthesis Kit protocol (Life Technologies), and then stored at −80 °C. Real-time PCR was performed using the PerfeCTa® qPCR FastMix® II, Low ROX™ (QuantaBio, cat # 97066–002) and off the shelf TaqMan gene expression assays from Life Technologies (Gria1, "GluR1", Mm00433753_m1; Gria2, "GluR2", Mm00442822_m1; Cnr1, "CB1", Mm01212171_s1; Grin1, "NR1", Mm00433790_m1; Grin2b, "NR2B″, Mm00433820_m1; Grm2, "mGluR2", Mm01235831_m1; Grm5, "mGluR5", Mm00690332_m1; Slc1a2, "GLT-1", Mm01275814_m1; Slc7a11, "xCT", Mm00442530_m1; Nr3c1, "GR", Mm00433832_m1; Nr3c2, "MR", Mm01241596_m1). For each sample, qPCR was run in triplicate on a Life Technologies/Applied Biosystems Viia7 real time PCR machine. Samples were compared using the ΔΔCt comparative quantification algorithms, with Rn18s (Mm04277571_s1) used as a housekeeping gene to normalize between biological replicates.

2.9. Surgery for in-vivo glutamate recordings

For implantation of cannula and head stages for glutamate measurements described in *Experiment 3*, mice were anaesthetized using 5% isoflurane in oxygen, and then maintained at 2% during the surgical procedure. Next, each mouse was prepared for electrophysiology measurements as previously described (Phillips et al., 2015; Wallace et al., 2020). Briefly, the skull surface was exposed and four stainless steel screw electrodes (Antrin Miniature Specialties, Inc. Fallbrook, CA) were implanted, along with two screws that were implanted in the parietal lobe to anchor the head stage. A guide cannula targeted to above the mPFC (bregma +1.90 mm A-P, +0.25 mm M-L, −0.75 mm D-V) was then implanted. These coordinates were selected as the biosensor protrudes from the base of the cannula an additional 1.8 mm, allowing for recording primarily from the prelimbic region of the mPFC. Two frontal electrodes were used to measure electroencephalogram (EEG), while two parietal electrodes were used as a reference and ground. These electrodes were soldered to a PCB headstage with a plastic 6-pin connector (Pinnacle Technology, Inc.). Two stainless steel wires attached to the PCB were inserted into the neck muscle to record electromyogram (EMG). The cannula, electrodes, and PCB were enclosed with a light activated flowable composite resin (Prime-Dent). Mice were then allowed at least 1 week recovery following surgery before the start of CORT treatment.

2.10. In-vivo glutamate recordings and analysis

Real-time glutamate measurements were made with an enzyme-based amperometric biosensor (Pinnacle). The electrode is a Teflon-coated 90% platinum–10% iridium (Pt–Ir) wire (Wakabayashi and Kiyatkin, 2012). Biologically plausible levels of ascorbic acid, dihydroxyphenylacetic acid, dopamine, serotonin, norepinephrine, homovanillic acid, methoxy-4-hydroxyphenylglycol, 5-hydroxyindoleacetic acid, L-tyrosine, L-cysteine, L-tryptophan, glutathione, uric acid, and catalase do not interfere with biosensor substrate detection (Hu et al., 1994; Naylor et al., 2011). Glutamate biosensors were purchased from Pinnacle Technology (cat. #7004) and pre-calibrated immediately before implantation using manufacturer specifications. Pre-calibration occurred in a jacketed beaker containing 20 mL 0.1 M phosphate buffered saline. Stepwise additions of 10 μM L-glutamate were made to the solution to verify biosensor sensitivity to L-glutamate, and a single addition of an interference solution (250 μM ascorbic acid) was made as a negative control to ensure specificity of the biosensor to L-glutamate. Following pre-calibration, biosensors were implanted into the mPFC and amperometric recordings were collected continuously at 1hz until the end of the experiment (see *Experiment 3* for details).

For analysis of biosensor recordings, raw data spanning the time period from −10 min (before start of stress) to 100 min (30 min of stress, plus 70 min of recovery) were first extracted and transformed in Matlab to remove artifacts before calculating and analyzing area under curve (AUC). For each biosensor recording, the data were transformed by excluding values in each recording outside the median ± interquartile range (to remove artifacts), and then each trace was normalized to the average of the 10-min baseline period preceding the start of stress exposure to determine change in glutamate during stress. Data traces were then combined by treatment group. For data analysis, AUC was calculated for all positive and negative peaks during the peri-stress recording period. To determine the specific changes in extracellular glutamate occurring during stress exposure (0–30min) vs after stress exposure (30–100min), AUC was then calculated for each time period separately. Cannula placements were verified after the experiment to ensure that all cannulae accurately targeted the mPFC. Some recordings were excluded from analysis (Control, N = 2; HPA-X, N = 1) due to poor quality of the recording trace.

2.11. Statistical analysis

For *Experiment 1*, two tailed Student's t tests were used to analyze gene data between Control and HPA-X groups for each gene of interest. For *Experiment 2*, two-way analyses of variance (ANOVA) were used to analyze FOS data (factors: stress x CORT treatment), with post hoc analyses undertaken using Tukey-corrected t-tests where appropriate. For *Experiment 3*, two tailed Student's t tests were used to analyze differences in AUC between groups. In all cases, tests for normality of distributions were included prior to statistical assessments. Results were considered significant at $p < 0.05$. All statistical analyses were undertaken using GraphPad Prism (version 7). In a handful of experiments, the number of samples analyzed differed from the number of samples run/collected. This is noted specifically in each figure caption. These data were not available due either to loss of the sample during processing (e.

g., not enough sample, poor RNA quality), or in the biosensor experiments, technical problems with the implanted sensor.

3. Results

3.1. HPA axis disruption alters expression of genes related to glutamate homeostasis in the mPFC, DG, and BLA

To determine the effects of chronic HPA axis disruption on glutamate homeostasis, we disrupted normal HPA function via chronic CORT treatment and quantified the expression of genes coding for ionotropic glutamate receptor subunits (GluR1, GluR2, NR1, NR2B), metabotropic glutamate receptors (mGluR2, mGlur5), astrocytic regulators of synaptic glutamate (GLT-1, xCT), and presynaptic regulators of synaptic excitability (CB1). We also quantified the expression of genes coding for glucocorticoid (GR) and mineralocorticoid (MR) receptors.

In the mPFC, we found that HPA-X mice had increased mRNA expression of ionotropic glutamate receptor subunits (GluR1, GluR2, NR1) as well as CB1 (Fig. 2). We also noted a trending increase in mGluR5 that did not reach statistical significance ($p = 0.052$). Overall, this pattern in changes of gene expression is consistent with an increase in postsynaptic excitability (GluR1, GluR2, NR1) and also an increase in presynaptic feedback inhibition to synaptic neurotransmitter release (CB1).

In the DG, we found that HPA-X mice had decreased mRNA expression of NMDA receptor subunits (NR1, NR2B), decreased expression of mGluR5, and decreased expression of astrocytic regulators of synaptic glutamate (GLT-1, xCT, Fig. 3). We also observed decreased GR and MR expression. Overall, this pattern of changes in mRNA expression is consistent with a decrease in postsynaptic excitability (NR1, NR2B, mGluR5), a decrease in synaptic glutamate buffering capacity (GLT-1), and a decrease in astrocyte mediated presynaptic inhibition (xCT).

In the BLA, we found that HPA-X mice had decreased mRNA expression of AMPA receptor subunit GluR1 and decreased expression of the astrocytic glutamate exchanger xCT (Fig. 4). Overall, these changes are consistent with a decrease in postsynaptic excitability (GluR1) and a decrease in astrocyte mediated presynaptic inhibition (xCT).

Together, our findings of mRNA expression changes suggest that chronic dysfunction of the HPA axis alters the balance of presynaptic, postsynaptic, and astrocytic regulators of glutamate homeostasis across the mPFC, DG, and BLA. However, the patterns of changes in gene expression vary between brain regions, suggesting different impacts of HPA disruption on neural function in each area.

3.2. HPA axis disruption alters stress-induced neural activation in the mPFC, but not the DG or BLA

To probe the functional consequences of changes in gene expression on neural activity, we disrupted normal HPA function and then exposed mice to an acute forced swim stress. Following stress exposure, we collected brain tissue and measured FOS immunoreactivity in the mPFC, DG, and BLA as a marker of neuronal activity (Fig. 5). We found that

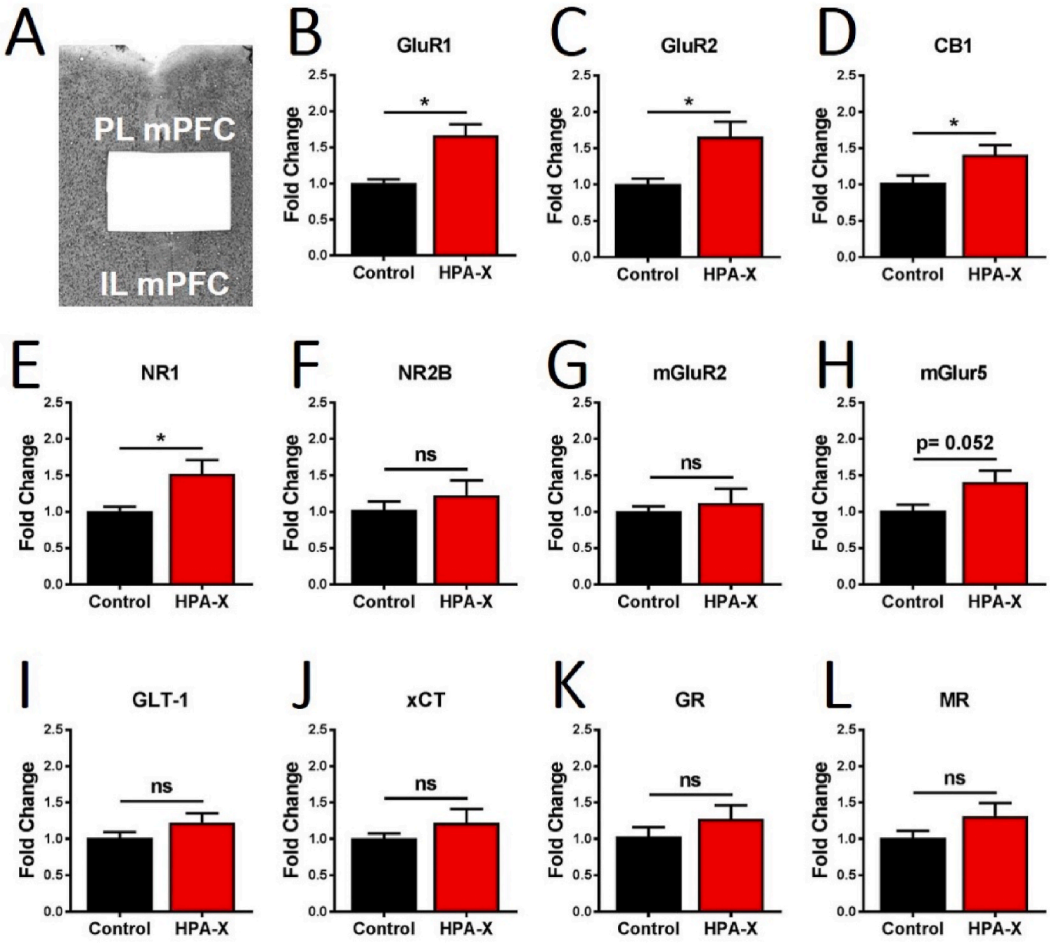

Fig. 2. mRNA expression results for the prelimbic medial prefrontal cortex (PL mPFC). (**A**) Example of laser microdissection of the PL mPFC. (**B-L**) Chronic HPA axis disruption with CORT increased the expression of GluR1 ($p = 0.003$), GluR2 ($p = 0.017$), CB1 ($p = 0.046$), and NR1 ($p = 0.034$), with a trend toward significance in mGluR5 ($p = 0.052$). Bars represent means +SEM; *$p < 0.05$, n = 6 (Control) and 7 (HPA-X). Two-tailed Student's *t* tests were used to compare differences between groups for each gene.

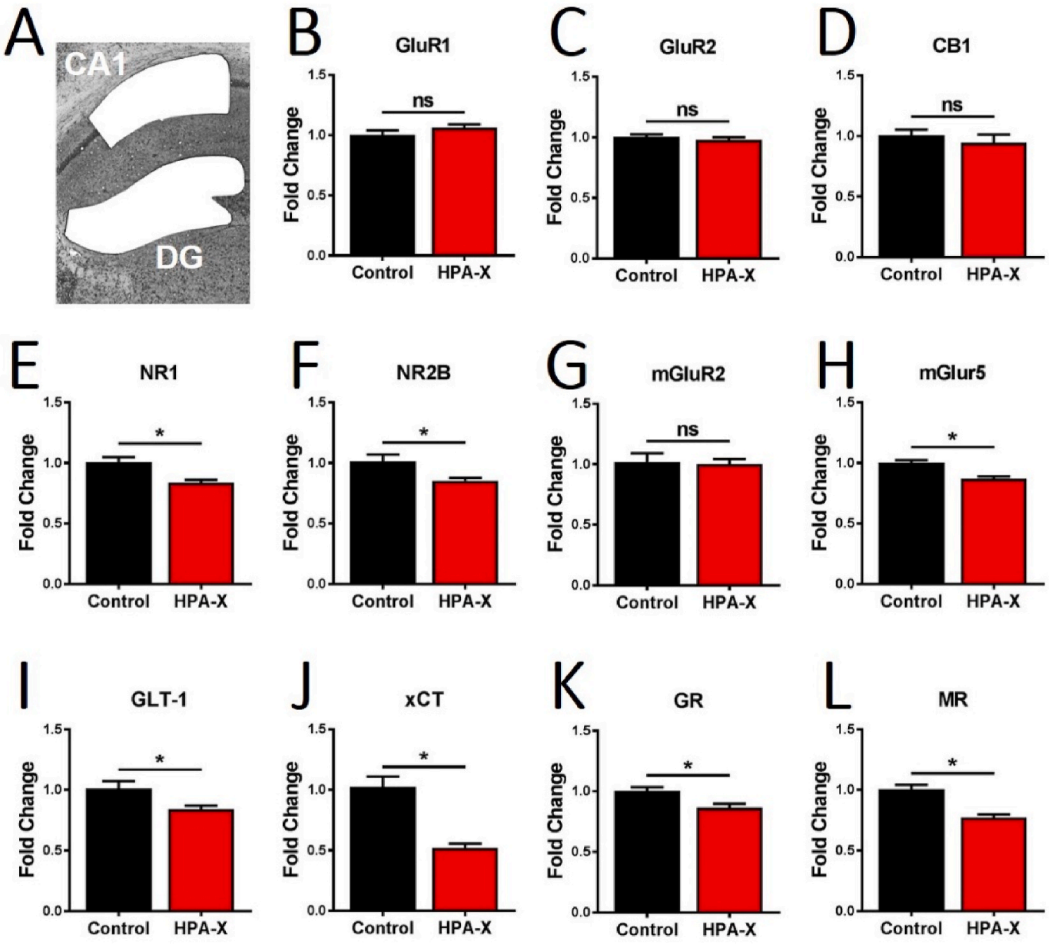

Fig. 3. mRNA expression results for the dentate gyrus of the hippocampus (DG). (**A**) Example of laser microdissection of the DG. (**B-L**) Chronic HPA axis disruption with CORT decreased the expression of NR1 ($p = 0.004$), NR2B ($p = 0.028$), mGluR5 ($p < 0.001$), GLT-1 ($p = 0.029$), xCT ($p < 0.001$), GR ($p = 0.006$), and MR ($p < 0.001$). Bars represent means +SEM; *$p < 0.05$, n = 8 mice/group. Two-tailed Student's *t* tests were used to compare differences between groups for each gene.

stress exposure increased FOS immunoreactivity in all three brain regions, however this response was significantly exaggerated in the mPFC of HPA-X mice. This suggests an increase in neuronal excitability in the mPFC following HPA disruption. However, the mechanisms by which this increase occurred remained unclear.

3.3. HPA axis disruption alters extracellular glutamate responses to acute stress in the mPFC

To further explore the causes of increased mPFC excitability following in HPA-X mice, we measured extracellular glutamate in the mPFC during exposure to acute immobilization stress following HPA axis disruption.

Our data show that during a restraint stress, extracellular glutamate detected by our biosensors decreases during stress in Control mice, and then shows a sustained increase following termination of the stress for up to 1-hr post stress (Fig. 6A). In HPA-X mice, a slight positive increase was observed, but overall the amount of change is very small compared to controls (Fig. 6A). This suggests a major change in the regulation of glutamate dynamics following HPA-X. To more clearly define these changes, we determined the absolute area under the curve (AUC) in both groups at different stages of the experiment. We found that HPA-X mice had decreased total extracellular glutamate flux during and after the stress exposure, as measured by total area under curve (Fig. 6B). We also found that absolute area under curve for extracellular glutamate was decreased during the stress period in HPA-X mice (Fig. 6C). Furthermore, we found that extracellular glutamate during the post-stress period was decreased in HPA-X mice (Fig. 6D). This suggests either less glutamate release from mPFC afferent neurons or an enhanced rate of glutamate clearance in the mPFC following stress. Together, these findings suggest that chronic HPA axis dysfunction decreases extracellular glutamate responses to stress in the mPFC.

4. Discussion

In the current study we investigated the impacts of chronic HPA axis dysfunction on glutamate homeostasis and neural responses to stress in three brain regions crucially linked to emotionality and stress-related neuropathology. Our results show that HPA disruption differentially alters the expression of genes related to glutamate homeostasis in the medial prefrontal cortex (mPFC), dentate gyrus of the hippocampus (DG), and basolateral amygdala (BLA). While gene expression was altered in all three regions, when challenged with stress exposure, there was an exaggeration of neural activation only in the mPFC. This suggested a greater functional consequence of HPA dysregulation on neural activity in the mPFC (at least in this measure). To probe the potential neurochemical underpinnings of this exaggerated activity, we measured extracellular glutamate in the mPFC in real time during stress exposure. We found that the dynamics of extracellular glutamate responses to stress were blunted in the mPFC. Our results show that chronic HPA axis disruption leads to alterations in the expression of different aspects of the glutamate signaling system in the mPFC, DG, and BLA.

Prefrontal Cortex: In the mPFC, we primarily observed an increase in the expression of genes related to postsynaptic excitability (GluR1,

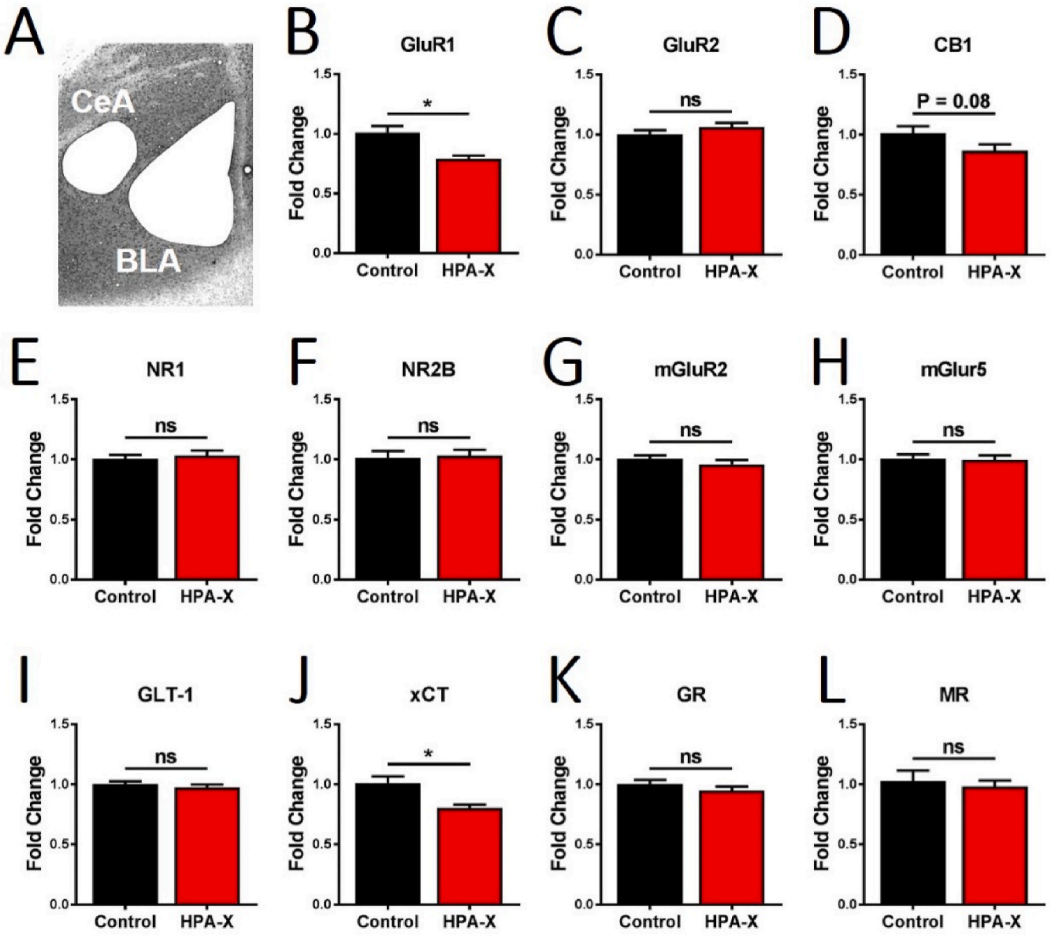

Fig. 4. mRNA expression results for the basolateral amygdala (BLA). (**A**) Example of laser microdissection of the BLA. (**B-L**) Chronic HPA axis disruption with CORT decreased the expression of GluR1 ($p = 0.003$) and xCT ($p = 0.005$), with a trending decrease in CB1 ($p = 0.076$). Bars represent means +SEM; *$p < 0.05$, n = 8 mice/group. Two-tailed Student's *t* tests were used to compare differences between groups for each gene. Central Amygdala (CeA) is shown only for anatomical orientation.

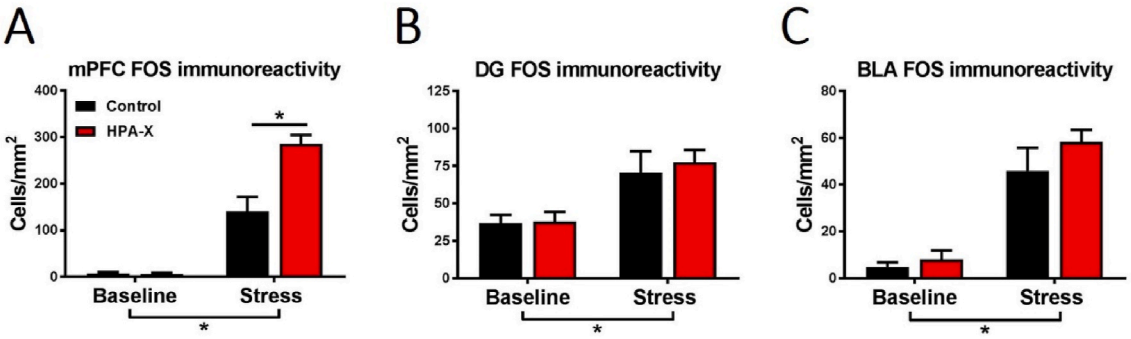

Fig. 5. FOS immunoreactivity, as measured by the number of FOS-positive nuclei per area of measure after a 10min swim stress. (**A**) mPFC FOS expression. We observe a main effect of stress ($F_{1, 27} = 128.7$, $p < 0.001$), CORT treatment ($F_{1, 27} = 15.62$, $p < 0.001$), and a significant interaction ($F_{1, 27} = 15.89$, $p < 0.001$). Stress increased mPFC FOS expression in both Control ($p < 0.001$) and HPA-X ($p < 0.001$) mice, however this increase was exaggerated in HPA-X mice ($p < 0.001$). (**B**) DG FOS expression. We observe a main effect of stress ($F_{1, 28} = 15.53$, $p < 0.001$), while no effect of CORT treatment was observed. Stress increased DG FOS expression in HPA-X mice ($p = 0.026$), with a trend toward significance in Control mice ($p = 0.072$). (**C**) BLA FOS expression. We observe a main effect of stress ($F_{1, 22} = 49.18$, $p < 0.001$), while no effect of CORT treatment was observed. Stress increased BLA FOS expression in both Control ($p < 0.001$) and HPA-X ($p < 0.001$) mice. Bars represent means +SEM; *$p < 0.05$. For the mPFC, n = 8 mice/stress condition (Control) and 7–8 mice/stress condition (HPA-X). For the DG, n = 8 mice/stress condition (Control and HPA-X). For the BLA, n = 6–7 mice/stress condition (Control) and 5–8 mice/stress condition (HPA-X). Two factor ANOVAs were used for each analysis with Tukey's *post-hoc* tests employed to probe interactions and perform individual comparisons between stress and treatment groups.

GluR2, NR1, mGluR5), but also observed an increase in CB1. This could be interpreted as an increase in the postsynaptic sensitivity to glutamate, or potentially as a compensatory response to reduced basal levels of extracellular glutamate in the mPFC. Aligned with the observed increased FOS response to stress following HPA disruption, this suggests that once stimulated by stress exposure, increased postsynaptic excitability to glutamate could cause an increase in activation of mPFC neurons.

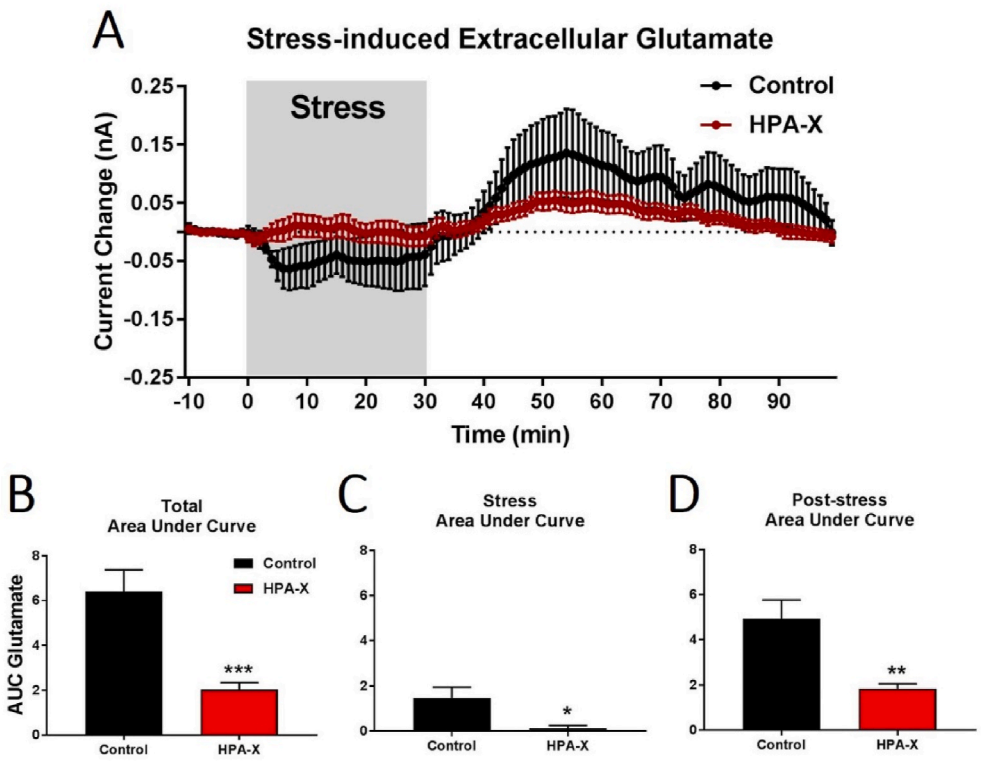

Fig. 6. Extracellular glutamate in the mPFC measured before, during, and after a 30min immobilization stress. (**A**) Plot of biosensor current change in the peri-stress period. Data traces are normalized relative to the 10min period before stress for each animal in the treatment group. (**B**) Total area under curve (AUC) using absolute values for the entirety of the peri-stress biosensor recording period. HPA-X mice had reduced total glutamate AUC compared to Control mice ($p < 0.001$). (**C**) AUC during only the stress period (0–30min) of the biosensor recording. HPA-X mice had reduced glutamate AUC during the stress period compared to Control mice ($p = 0.011$). (**D**) AUC during only the post-stress period (30–100min) of the biosensor recording. HPA-X mice had reduced glutamate AUC during the post-stress period compared to Control mice ($p = 0.002$). Bars and biosensor traces represent means ± SEM; *$p < 0.05$, n = 8 (Control) and 9 (HPA-X). Two-tailed Student's *t* tests were used to compare differences in AUC between groups.

Hippocampus: In the DG, we observed downregulation in the expression of genes related to postsynaptic excitability (NR1, NR2B, mGluR5), astrocytic glutamate regulators (GLT-1, xCT), and glucocorticoid sensitivity (GR, MR) in HPA-X mice. These changes could be interpreted as decreased postsynaptic sensitivity to glutamate and decreased ability to maintain synaptic glutamate levels. The DG is a site of neurogenesis throughout the lifespan and is sensitive to stress and glucocorticoid exposure (Kim et al., 2015; Gould and Tanapat, 1999). Indeed, this is evidenced by decreased GR and MR expression in HPA-X mice, which were not observed in the mPFC or BLA. However, despite these changes in gene expression we observed no difference in basal or stress-induced FOS responses in the DG after HPA disruption. Notably, we previously showed an increase in stress-induced *c-fos* mRNA expression in tissue punches from the dorsal and ventral hippocampus after HPA disruption (Kinlein et al., 2015), suggesting that these effects may be subregion-specific. It will be important for future studies to test how the changes in gene expression caused by HPA disruption relate to structural plasticity or circuit function in the DG and throughout the hippocampus, and the behavioral consequences of any observed changes. It is possible that decreased astrocytic control of extracellular glutamate by GLT-1 and xCT lead to excessive synaptic glutamate concentrations, which causes a compensatory decrease in NMDA receptor function to reduce excitotoxicity. Furthermore, it will be important to explore effects on the ventral DG and other sub-regions of the hippocampus.

Amygdala: In the BLA, we found that HPA disruption led to downregulation of genes related to postsynaptic (GluR1) and presynaptic (CB1, xCT) excitability. However, as in the DG, despite these effects, we observed no change in basal or stress-induced FOS in the BLA. These results suggest that this model of chronic HPA dysfunction may affect glutamatergic tone in the BLA, but also that these changes are not sufficient to lead to changes in neuronal excitability. Importantly, GABA signaling appears to be crucial for BLA circuit function (Jie et al., 2018; Bhatnagar et al., 2004; Prager et al., 2016), so it will also be necessary to determine if HPA disruption affects GABAergic signaling in the BLA, and whether this leads to changes in structural or functional plasticity.

The mPFC, hippocampus, and amygdala have been well studied for their roles in control of the HPA axis response to stress, and their links to stress-related disease (McEwen et al., 2015, 2016). The mPFC and hippocampus exert glucocorticoid-dependent negative feedback inhibition to the HPA axis through glutamatergic projections to the posterior region of the bed nucleus of the stria terminalis (pBST) (Crestani et al., 2013). In contrast, the amygdala is thought to stimulate HPA axis activity through GABAergic projections from the CeA to the BST (Herman et al., 2016; Ulrich-Lai and Herman, 2009; Crestani et al., 2013). The BST sends mostly GABAergic projections to the PVN, leading to the hypothesis that the overall contributions of these regions to HPA axis activity and autonomic function occur through this common relay point (Ulrich-Lai and Herman, 2009; Crestani et al., 2013). That the BST shares projections from all these regions makes it a prime candidate for future studies examining the effects of HPA dysfunction on mPFC, hippocampus, and amygdala circuit activity. In addition to circuits involving the HPA axis, these regions are linked with direct and indirect projections to one another. While many multi-synaptic connections between the prefrontal cortex and hippocampus have been established, there are direct monosynaptic projections from the CA1 and subiculum to the mPFC, terminating in the anterior cingulate, prelimbic, and infralimbic cortices (Cenquizca and Swanson, 2007; Chiba, 2000; Godsil et al., 2013). Additionally, the hippocampus shares direct connections with the BLA, and the prelimbic and infralimbic sub-regions of the mPFC share bidirectional glutamatergic projections with the BLA (Orsini et al., 2011; Riga et al., 2014; Vertes, 2004). Given the connections between these brain regions, our findings suggest that alterations in glutamate homeostasis following HPA disruption may alter function of these circuits, and under stressful conditions this could lead to changes in the behavioral and emotional processes engaged by the organism.

Our FOS results suggest that although HPA disruption altered the expression of genes related to glutamate signaling in the DG and BLA, this may not result in a net change in stress-induced neuronal activity in these regions. However, in the mPFC, we found that stress resulted in exaggerated mPFC FOS responses in HPA-X mice. This indicates that chronic HPA disruption alters mPFC neuronal sensitivity to stimulation

by stress. This increase in mPFC activity could be due to increased postsynaptic sensitivity to glutamate release, increased glutamate release, or a decrease in inhibitory tone in this area. Our gene expression data support the notion that postsynaptic sensitivity is likely increased after HPA disruption, as we observed increases in the expression of AMPA (*GluR1, GluR2*) and NMDA (*NR1*) receptor subunits. We have not yet explored the effects of HPA disruption on expression of genes related to GABAergic signaling, however decreases in inhibitory signaling could contribute to the increased FOS responses observed. It is well established in both humans and rodents that chronic stress leads to dysfunction of the mPFC (McEwen and Morrison, 2013; McEwen et al., 2015; Goldwater et al., 2009). One hypothesis for this phenomenon is that decreased dendritic complexity caused by chronic stress results in decreased synaptic excitability between neurons in the mPFC (McEwen et al., 2015, 2016; Goldwater et al., 2009). Additionally, there is an increase in inhibitory tone in the mPFC following chronic stress exposure (McKlveen et al., 2016). Both ideas are consistent with responses that may arise to resist excessive excitation by glutamate. As our results show HPA dysregulation contributes to increased mPFC excitability following acute stress, this could indicate that changes in mPFC responses following chronic stress would be accelerated or potentiated in this model. This hypothesis needs to be tested in future studies.

To further understand the mechanisms by which HPA disruption altered mPFC activity, we measured extracellular glutamate in real time before, during, and after stress exposure. While prior studies have examined *in vivo* stress-induced glutamate release, this has traditionally been accomplished using HPLC following microdialysis (Lowy et al., 1993, 1995; Moghaddam et al., 1994; Stein-Behrens et al., 1994; Bagley and Moghaddam, 1997; Macht et al., 2020). The microdialysis procedure consists of perfusing a brain region of interest with buffer solution, then collecting samples, including the analyte of interest, via diffusion through a semipermeable membrane (Chefer et al., 2009). While the microdialysis approach is clearly superior to our biosensor approach in terms of quantification of analyte concentrations, two major drawbacks of microdialysis are sampling rate (typically >1min), and analyte depletion from the area of interest (Chefer et al., 2009). In this study, we used enzymatic amperometric biosensors which have a much faster sampling rate (1hz) and do not require the removal of analyte from the brain for sampling (Wilson and Gifford, 2005; Wilson and Johnson, 2008; Moore et al., 2019; Siemsen et al., 2020). However, a drawback of this technique is the inability to measure absolute concentrations of analyte, which limits interpretations of the data to that of relative changes within a recording. Our results show that during immobilization stress in Control mice, extracellular glutamate concentrations exhibit a decrease immediately upon stress exposure, and then show a sustained increase at the end of stress exposure until returning to baseline levels around 60-min after the cessation of stress. In contrast, we observed reduced glutamate fluctuations both during and after stress exposure in HPA-X mice. This suggests dysregulation in afferent glutamate release and/or mechanisms of synaptic glutamate clearance in HPA-X mice. Previous microdialysis studies have shown that acute stress increases extracellular glutamate in the mPFC and hippocampus (Lowy et al., 1993, 1995; Moghaddam et al., 1994; Bagley and Moghaddam, 1997; Macht et al., 2020; Lupinsky et al., 2010). However, in previous studies with mPFC glutamate measures, glutamate rose very quickly after stress onset (within 30 min), while we observe a decrease in glutamate immediately following stress onset.

Our finding of decreased extracellular glutamate at stress onset, and then a delayed yet sustained increase following stress termination was unexpected. We are only able to speculate that these differences in glutamate responses to stress could be driven by experimental and/or technical aspects. For instance, we can conjecture that pain from the tail pinch method used in Bagley et al. (1997) is certainly one potential variable that should be considered, given we used an immobilization stressor that does not involve pain. That said, Macht et al. (2020), who used a 1-h long immobilization stress (similar to our stressor), found an increase in PFC glutamate by about 15–30-min into the stressor. However, Macht et al. (2020) used a sampling rate of 15-min, while we used a 1-s sampling rate, and our stressor was much shorter (30-min versus 60-min). It is intriguing to speculate that it is possible the increase we observed following stress termination is in fact part of the normal response to a stress onset, an outcome that aligns well with the subsequent time points in Macht et al. (2020). In addition to this conjecture, notable technical considerations are the surgical and acclimation procedure used prior to glutamate measurement. In most previous studies, surgical manipulations were performed only 24-h to 7-days prior to glutamate measurement (and most occur within 72-h). In contrast, in our study surgical manipulations were performed 5-weeks prior to glutamate measurements. It is possible that effects of surgical pain or inflammation at the site of cannula placement affected observations in prior studies, as processes of reactive gliosis and tissue damage can persist for up to two weeks after focal damage in the central nervous system (Burda and Sofroniew, 2014). Importantly, these brain inflammatory responses can have a significant impact on the regulation of extracellular glutamate levels (Haroon et al., 2017; Takeuchi et al., 2006). With regards to habituation and day-of-testing differences, in previous studies animals were housed in home cages until the day of testing, or with minimal habituation (e.g. 4–5 h each day) to the recording apparatus, when perfusion and sample collection through the microdialysis probe began (Moghaddam et al., 1994; Bagley and Moghaddam, 1997; Lupinsky et al., 2010). However, our mice were acclimated (including tethering to preamplifier boxes) for at least 42-h in the testing chamber. Importantly, as biosensor current can be measured without a need to collect physical samples, mice were not disturbed on the day of testing until the start of stress exposure. Thus, it is possible that the technical procedures required for microdialysis sampling (e.g. re-housing and handling) introduce additional stress to the animal, and this may affect the baseline and stress-induced dynamics of mPFC glutamate release.

As a possible mechanistic explanation of decreased glutamate in the current study, Lupinsky et al. (2010) showed that intra-mPFC administration of an $mGluR_{2/3}$ receptor agonist caused acute tail-pinch stress to decrease, rather than increase extracellular glutamate concentrations (Lupinsky et al., 2010). Thus, it is possible that presynaptic metabotropic glutamate receptors mediate the initial decrease in glutamate observed in the current study. Nevertheless, it is noteworthy that the initial decrease in mPFC glutamate did not occur in HPA-X mice, which fully support our conclusion that HPA disruption altered mechanisms of dynamic stress-induced glutamate regulation om the mPFC.

There are multiple mechanisms which could underlie reduced fluctuations in stress-induced extracellular glutamate levels in HPA-X mice. Our gene expression results from the mPFC showed an increase in *CB1* expression in HPA-X mice, indicating a possible endocannabinoid-mediated mechanism by which the presynaptic release of glutamate could be reduced during stress. Furthermore, previous microdialysis studies showed that adrenalectomy (ADX) attenuated stress-induced extracellular glutamate increases in the mPFC and hippocampus (Lowy et al., 1993; Moghaddam et al., 1994), suggesting a role of glucocorticoids in these responses. However, while ADX prevented the increase in extracellular glutamate in the hippocampus, this reduction was less pronounced in the mPFC (Moghaddam et al., 1994). This suggests that the sufficiency of glucocorticoids to increase glutamate release during stress may be brain region-dependent. Importantly, as extracellular glutamate concentrations change within 15–20-min following stress onset in the above studies, this suggests that any effects of glucocorticoids would be mediated by rapid effects on synaptic function rather than effects dependent on gene transcription.

5. Caveats, considerations, and future directions

That our study does not include female mice is a clear caveat. Given the extant (and growing) understanding of the importance of including

sex as a biological variable (Shansky and Murphy, 2021), particularly in stress research (Shansky and Woolley, 2016), it will be important to understand how these responses may (or may not) differ between sex. With specific regard to stress, understanding how these differences might manifest on the behavioral and circuit levels is of significant import, and future work should consider new data on differences in stress responses between males and females (Baratta et al., 2019; Colom-Lapetina et al., 2019) as part of any experimental design. Our findings of decreased stress-induced glutamate levels in HPA-X mice were surprising given that we observed increased stress-induced mPFC FOS in this group. However, there are several things to consider when comparing these results. First, two different stressors were used. While we could not perform glutamate recordings during swim stress due to technical considerations, it would be useful to know how stressor modality affects the relationship between mPFC glutamate levels and overall neural activity in the region. While we attempted to undertake our biosensor measures during the same swim stress we used in the FOS experiment, it was technically unfeasible. Switching to immobilization stress for our glutamate measures precludes direct comparison to the FOS experiment, but does not change the interpretation of the gene expression data which are from baseline non-stressed mice. Finally, in addition to effects of glutamate on neuronal excitability, other neurotransmitter systems have been shown to affect mPFC function. For example, $5HT_{2A/2C}$ receptor agonists and dopamine D1/D2 antagonists alone are sufficient to increase mPFC FOS in the absence of stress (Benneyworth et al., 2007; Perreault et al., 2015). It will be necessary to determine the effects of HPA disruption on these neurotransmitter systems to fully determine the impacts on mPFC, hippocampus, and amygdala circuit function and the implications for behavioral and emotional responses to stress. Finally, we have previously shown that while time spent struggling in the FST in HPA-X mice is not statistically different, "coping behaviors" are altered following FST in HPA-X mice (Kinlein et al., 2015). Thus, it is possible coping behaviors during the stressor might be different in different stressor modalities (e.g., swim vs. immobilization). While such a comparison is beyond the scope of the present work, it is certainly possible that HPA-x changed the stressor modality specific coping behaviors.

6. Conclusions

This study shows that chronic HPA dysfunction induces adaptation in the glutamate signaling system across multiple brain regions, which coincides with altered stress-induced glutamate responses and neural activation in the mPFC. While neural responses to acute stress in the hippocampus and amygdala were not affected in our model of HPA dysfunction, we observed an exaggerated response to stress in the mPFC as measured by FOS expression. Furthermore, the dynamics of extracellular glutamate responses to stress were blunted in the mPFC, suggesting that HPA dysfunction compromises normal function of this brain region under conditions of stress.

While strong links have been made between chronic HPA dysregulation and the development of stress-related psychiatric disorders, the mechanisms by which chronic HPA dysfunction affects communication and synaptic function in the brain likely involve many different cell-signaling systems across different brain regions. Further studies will be needed to determine how glucocorticoids and other endocrine signals mediate the brain-wide response to stress as a whole, and the consequences for these changes on behavior.

Funding

This work was supported by an NSF CAREER Award (1553067) and an NIH R01DK119811 to INK, as well as a Poncin Foundation Fellowship to SAK.

Declaration of competing interest

The authors declare that they have no known competing financial interests or personal relationships that could have appeared to influence the work reported in this paper.

CRediT authorship contribution statement

Scott A. Kinlein: Conceptualization, Methodology, Formal analysis, Resources, Investigation, Visualization, Writing – original draft. **Naomi K. Wallace:** Investigation, Resources. **Marina I. Savenkova:** Methodology, Formal analysis, Investigation, Resources. **Ilia N. Karatsoreos:** Conceptualization, Methodology, Formal analysis, Investigation, Writing – original draft, Supervision, Project administration, Funding acquisition.

Data availability

Data will be made available on request.

Acknowledgement

The authors would like to acknowledge the tremendous contributions of Dr. Bruce McEwen to the field of stress neurobiology, physiology and behavior, which certainly would not have taken its current form without his scientific insights and personal dedication to discovery. His enduring impact on the field is amplified because of his mentorship, both formal and informal, of dozens of postdoctoral fellows, graduate students, and principal investigators over his long career (including both the first and senior author of this manuscript). It is hoped that we all can continue the tradition of scientific generosity, humility and decency that Dr. Bruce McEwen brought to the field each and every day.

References

Bagley, J., Moghaddam, B., 1997. Temporal dynamics of glutamate efflux in the prefrontal cortex and in the hippocampus following repeated stress: effects of pretreatment with saline or diazepam. Neuroscience 77, 65–73.
Baratta, M.V., et al., 2019. Controllable stress elicits circuit-specific patterns of prefrontal plasticity in males, but not females. Brain Struct. Funct. 224, 1831–1843.
Benneyworth, M.A., et al., 2007. A selective positive allosteric modulator of metabotropic glutamate receptor subtype 2 blocks a hallucinogenic drug model of psychosis. Mol. Pharmacol. 72, 477–484.
Bhatnagar, S., Vining, C., Denski, K., 2004. Regulation of chronic stress-induced changes in hypothalamic-pituitary-adrenal activity by the basolateral amygdala. Ann. N. Y. Acad. Sci. 1032, 315–319.
Bose, M., Olivan, B., Laferrere, B., 2009. Stress and obesity: the role of the hypothalamic-pituitary-adrenal axis in metabolic disease. Curr. Opin. Endocrinol. Diabetes Obes. 16, 340–346.
Burda, J.E., Sofroniew, M.V., 2014. Reactive gliosis and the multicellular response to CNS damage and disease. Neuron 81, 229–248.
Cenquizca, L.A., Swanson, L.W., 2007. Spatial organization of direct hippocampal field CA1 axonal projections to the rest of the cerebral cortex. Brain Res. Rev. 56, 1–26.
Chefer, V.I., Thompson, A.C., Zapata, A., Shippenberg, T.S., 2009. Overview of Brain Microdialysis. Current Protocols in Neuroscience/Editorial Board, Jacqueline N. Crawley [et al.] (Chapter 7), Unit7 1.
Chiba, T., 2000. Collateral projection from the amygdalo–hippocampal transition area and CA1 to the hypothalamus and medial prefrontal cortex in the rat. Neurosci. Res. 38, 373–383.
Colom-Lapetina, J., Li, A.J., Pelegrina-Perez, T.C., Shansky, R.M., 2019. Behavioral diversity across classic rodent models is sex-dependent. Front. Behav. Neurosci. 13, 45.
Crestani, C.C., et al., 2013. Mechanisms in the bed nucleus of the stria terminalis involved in control of autonomic and neuroendocrine functions: a review. Curr. Neuropharmacol. 11, 141–159.
Datson, N.A., Morsink, M.C., Meijer, O.C., de Kloet, E.R., 2008. Central corticosteroid actions: search for gene targets. Eur. J. Pharmacol. 583, 272–289.
de Kloet, C.S., et al., 2006. Assessment of HPA-axis function in posttraumatic stress disorder: pharmacological and non-pharmacological challenge tests, a review. J. Psychiatr. Res. 40, 550–567.
Dedovic, K., Ngiam, J., 2015. The cortisol awakening response and major depression: examining the evidence. Neuropsychiatric Dis. Treat. 11, 1181–1189.
Erecinska, M., Silver, I.A., 1990. Metabolism and role of glutamate in mammalian brain. Prog. Neurobiol. 35, 245–296.

Franklin, K.B.J., Paxinos, G., 2007. The Mouse Brain in Stereotaxic Coordinates. Academic Press.
Godsil, B.P., Kiss, J.P., Spedding, M., Jay, T.M., 2013. The hippocampal-prefrontal pathway: the weak link in psychiatric disorders? Eur. Neuropsychopharmacol : the journal of the European College of Neuropsychopharmacology 23, 1165–1181.
Goldwater, D.S., et al., 2009. Structural and functional alterations to rat medial prefrontal cortex following chronic restraint stress and recovery. Neuroscience 164, 798–808.
Gould, E., Tanapat, P., 1999. Stress and hippocampal neurogenesis. Biol. Psychiatr. 46, 1472–1479.
Harbuz, M., 2002. Neuroendocrinology of autoimmunity. Int. Rev. Neurobiol. 52, 133–161.
Haroon, E., Miller, A.H., Sanacora, G., 2017. Inflammation, glutamate, and glia: a trio of trouble in mood disorders. Neuropsychopharmacology : official publication of the American College of Neuropsychopharmacology 42, 193–215.
Herman, J.P., et al., 2016. Regulation of the hypothalamic-pituitary-adrenocortical stress response. Compr. Physiol. 6, 603–621.
Hu, Y., Mitchell, K.M., Albahadily, F.N., Michaelis, E.K., Wilson, G.S., 1994. Direct measurement of glutamate release in the brain using a dual enzyme-based electrochemical sensor. Brain Res. 659, 117–125.
Jie, F., et al., 2018. Stress in regulation of GABA amygdala system and relevance to neuropsychiatric diseases. Front. Neurosci. 12, 562.
Joels, M., Sarabdjitsingh, R.A., Karst, H., 2012. Unraveling the time domains of corticosteroid hormone influences on brain activity: rapid, slow, and chronic modes. Pharmacol. Rev. 64, 901–938.
Kim, E.J., Pellman, B., Kim, J.J., 2015. Stress effects on the hippocampus: a critical review. Learn. Mem. 22, 411–416.
Kinlein, S.A., Wilson, C.D., Karatsoreos, I.N., 2015. Dysregulated hypothalamic-pituitary-adrenal axis function contributes to altered endocrine and neurobehavioral responses to acute stress. Front. Psychiatr. 6, 31.
Lowy, M.T., Gault, L., Yamamoto, B.K., 1993. Adrenalectomy attenuates stress-induced elevations in extracellular glutamate concentrations in the hippocampus. J. Neurochem. 61, 1957–1960.
Lowy, M.T., Wittenberg, L., Yamamoto, B.K., 1995. Effect of acute stress on hippocampal glutamate levels and spectrin proteolysis in young and aged rats. J. Neurochem. 65, 268–274.
Lupinsky, D., Moquin, L., Gratton, A., 2010. Interhemispheric regulation of the medial prefrontal cortical glutamate stress response in rats. J. Neurosci. : the official journal of the Society for Neuroscience 30, 7624–7633.
Luscher, C., Malenka, R.C., 2012. NMDA receptor-dependent long-term potentiation and long-term depression (LTP/LTD). Cold Spring Harbor Perspect. Biol. 4.
Macht, V.A., et al., 2020. Interactions between pyridostigmine bromide and stress on glutamatergic neurochemistry: insights from a rat model of Gulf War Illness. Neurobiology of Stress 12, 100210.
McEwen, B.S., 1998. Stress, adaptation, and disease. Allostasis and allostatic load. Ann. N. Y. Acad. Sci. 840, 33–44.
McEwen, B.S., Morrison, J.H., 2013. The brain on stress: vulnerability and plasticity of the prefrontal cortex over the life course. Neuron 79, 16–29.
McEwen, B.S., et al., 2015. Mechanisms of stress in the brain. Nat. Neurosci. 18, 1353–1363.
McEwen, B.S., Nasca, C., Gray, J.D., 2016. Stress effects on neuronal structure: Hippocampus, amygdala, and prefrontal cortex. Neuropsychopharmacology : official publication of the American College of Neuropsychopharmacology 41, 3–23.
McKlveen, J.M., et al., 2016. Chronic stress increases prefrontal inhibition: a mechanism for stress-induced prefrontal dysfunction. Biol. Psychiatr. 80, 754–764.
Meldrum, B.S., 2000. Glutamate as a neurotransmitter in the brain: review of physiology and pathology. J. Nutr. 130, 1007S–15S.
Moghaddam, B., Bolinao, M.L., Stein-Behrens, B., Sapolsky, R., 1994. Glucocorticoids mediate the stress-induced extracellular accumulation of glutamate. Brain Res. 655, 251–254.
Moore, K.M., et al., 2019. Glutamate afferents from the medial prefrontal cortex mediate nucleus accumbens activation by female sexual behavior. Front. Behav. Neurosci. 13.
Musazzi, L., Treccani, G., Popoli, M., 2012. Glutamate hypothesis of depression and its consequences for antidepressant treatments. Expert Rev. Neurother. 12, 1169–1172.
Naylor, E., et al., 2011. Simultaneous real-time measurement of EEG/EMG and L-glutamate in mice: a biosensor study of neuronal activity during sleep. J. Electroanal. Chem. 656, 106–113.
Orsini, C.A., Kim, J.H., Knapska, E., Maren, S., 2011. Hippocampal and prefrontal projections to the basal amygdala mediate contextual regulation of fear after extinction. J. Neurosci. : the official journal of the Society for Neuroscience 31, 17269–17277.
Pariante, C.M., Lightman, S.L., 2008. The HPA axis in major depression: classical theories and new developments. Trends Neurosci. 31, 464–468.
Perreault, M.L., Shen, M.Y., Fan, T., George, S.R., 2015. Regulation of c-fos expression by the dopamine D1-D2 receptor heteromer. Neuroscience 285, 194–203.
Phillips, D.J., Savenkova, M.I., Karatsoreos, I.N., 2015. Environmental disruption of the circadian clock leads to altered sleep and immune responses in mouse. Brain Behav. Immun. 47, 14–23.
Popoli, M., Yan, Z., McEwen, B.S., Sanacora, G., 2011. The stressed synapse: the impact of stress and glucocorticoids on glutamate transmission. Nat. Rev. Neurosci. 13, 22–37.
Prager, E.M., Bergstrom, H.C., Wynn, G.H., Braga, M.F., 2016. The basolateral amygdala gamma-aminobutyric acidergic system in health and disease. J. Neurosci. Res. 94, 548–567.
Ressler, K.J., 2010. Amygdala activity, fear, and anxiety: modulation by stress. Biol. Psychiatr. 67, 1117–1119.
Riga, D., et al., 2014. Optogenetic dissection of medial prefrontal cortex circuitry. Front. Syst. Neurosci. 8, 230.
Sanacora, G., Treccani, G., Popoli, M., 2012. Towards a glutamate hypothesis of depression: an emerging frontier of neuropsychopharmacology for mood disorders. Neuropharmacology 62, 63–77.
Shahanoor, Z., Sultana, R., Baker, M.R., Romeo, R.D., 2017. Neuroendocrine stress reactivity of male C57BL/6N mice following chronic oral corticosterone exposure during adulthood or adolescence. Psychoneuroendocrinology 86, 218–224.
Shansky, R.M., Murphy, A.Z., 2021. Considering sex as a biological variable will require a global shift in science culture. Nat. Neurosci. 24, 457–464.
Shansky, R.M., Woolley, C.S., 2016. Considering sex as a biological variable will Be valuable for neuroscience research. J. Neurosci. 36, 11817–11822.
Siemsen, B.M., et al., 2020. Amperometric measurements of cocaine cue and novel context-evoked glutamate and nitric oxide release in the nucleus accumbens core. J. Neurochem. 153, 599–616.
Stein-Behrens, B.A., Lin, W.J., Sapolsky, R.M., 1994. Physiological elevations of glucocorticoids potentiate glutamate accumulation in the hippocampus. J. Neurochem. 63, 596–602.
Takeuchi, H., et al., 2006. Tumor necrosis factor-alpha induces neurotoxicity via glutamate release from hemichannels of activated microglia in an autocrine manner. J. Biol. Chem. 281, 21362–21368.
Ulrich-Lai, Y.M., Herman, J.P., 2009. Neural regulation of endocrine and autonomic stress responses. Nat. Rev. Neurosci. 10, 397–409.
Vertes, R.P., 2004. Differential projections of the infralimbic and prelimbic cortex in the rat. Synapse 51, 32–58.
Wakabayashi, K.T., Kiyatkin, E.A., 2012. Rapid changes in extracellular glutamate induced by natural arousing stimuli and intravenous cocaine in the nucleus accumbens shell and core. J. Neurophysiol. 108, 285–299.
Wallace, N.K., Pollard, F., Savenkova, M., Karatsoreos, I.N., 2020. Effect of aging on daily rhythms of Lactate metabolism in the medial prefrontal cortex of male mice. Neuroscience 448, 300–310.
Wilson, G.S., Gifford, R., 2005. Biosensors for real-time in vivo measurements. Biosens. Bioelectron. 20, 2388–2403.
Wilson, G.S., Johnson, M.A., 2008. In-vivo electrochemistry: what can we learn about living systems? Chem. Rev. 108, 2462–2481.